

ROTATING AND STATIONARY RECTANGULAR COOLING PASSAGES

HEAT TRANSFER AND FRICTION WITH TURBULATORS, PINS AND DIMPLES

J.C. Han

Mechanical Engineering
Texas A&M University
College Station, TX 77843

Phil Ligrani

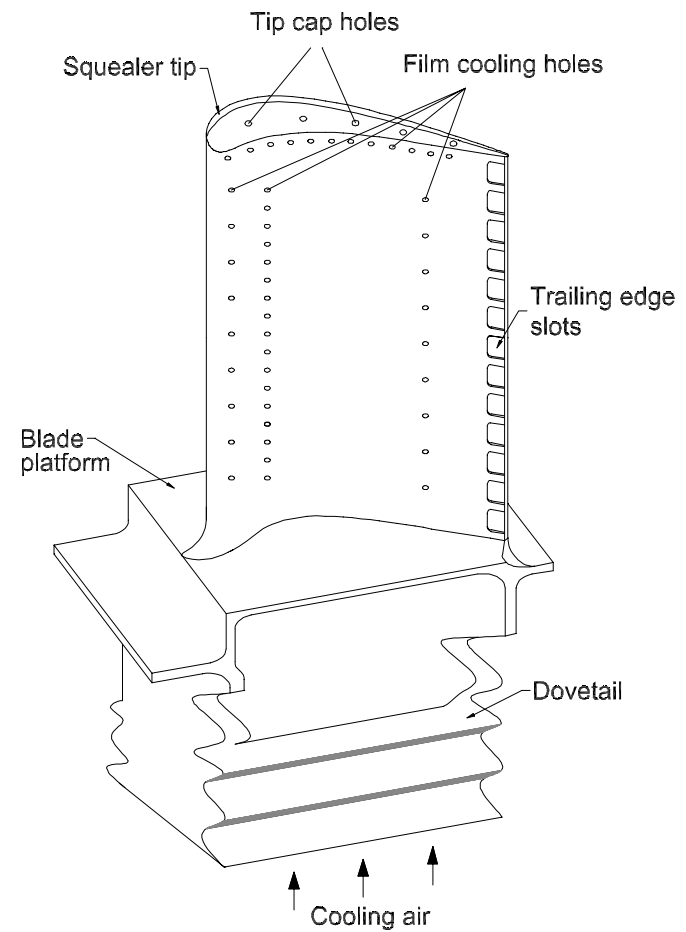
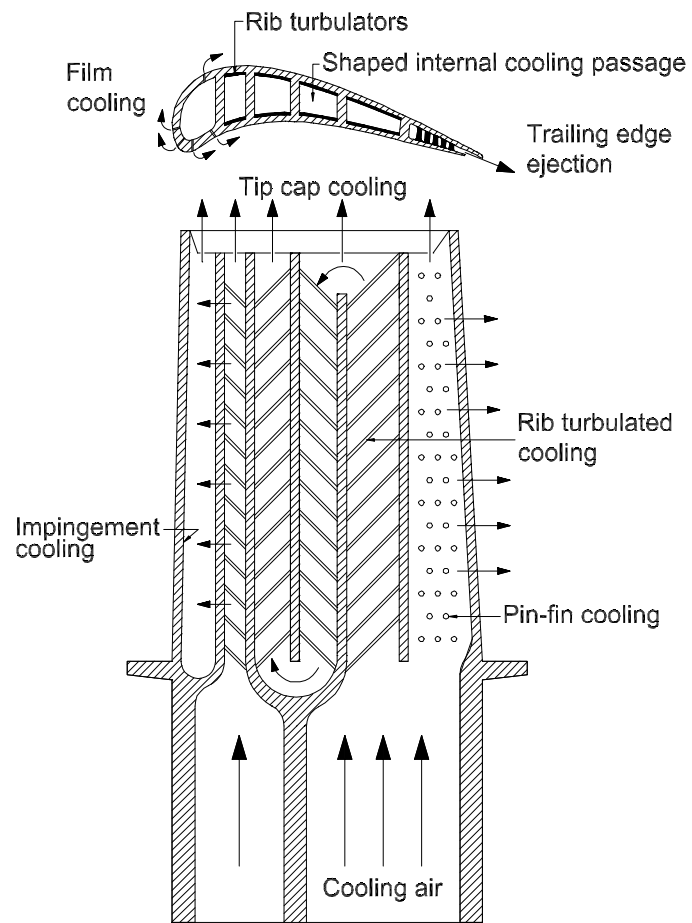
Mechanical Engineering
University of Utah
Salt Lake City, UT 84112

H.C. Chen

Civil Engineering
Texas A&M University
College Station, TX 77843

presentation at
Turbine Power Systems Conference and Condition Monitoring Workshop
Moody Gardens Hotel
Galveston, Texas
February 25-27, 2002

Gas Turbine Heat Transfer and Cooling Technology

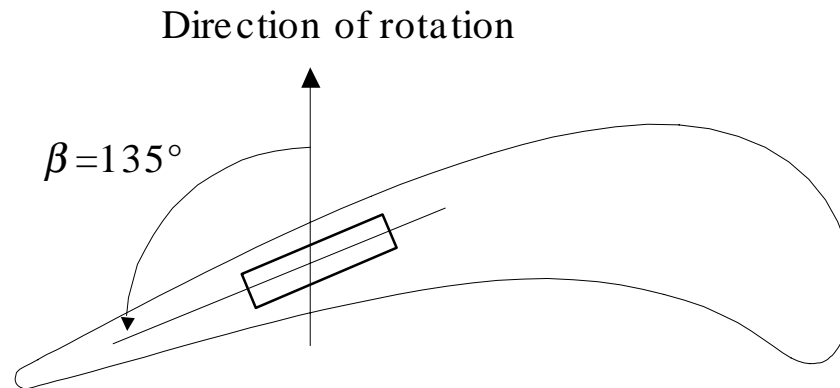


The Project Contains Three Parts Spanning Two Years -

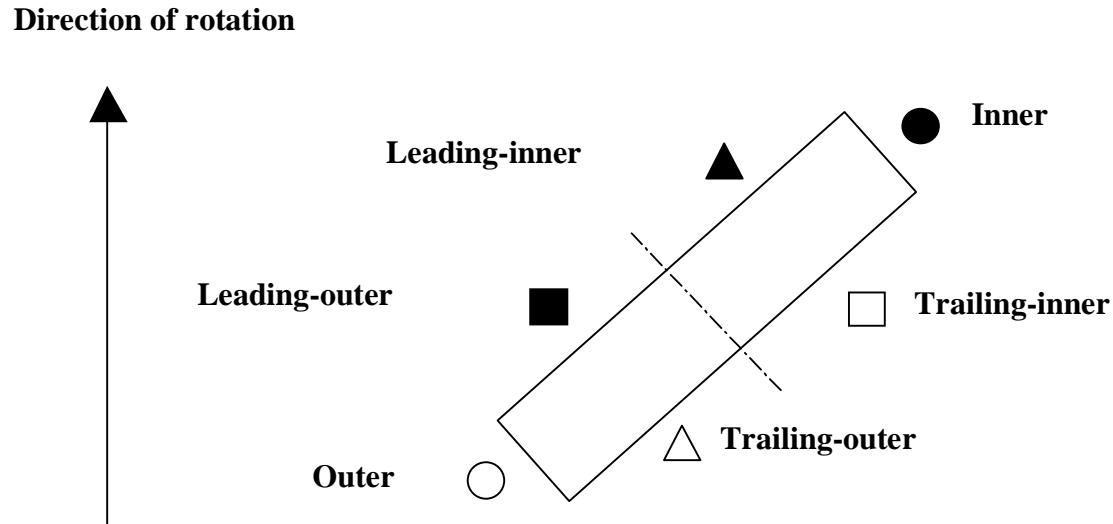
Focus is on Heat Transfer in Rectangular Cooling Passages (near a blade's trailing edge region) with Ribs, Pins and Dimples

- Part I: Rotating Heat Transfer: Focuses on the effects of rotation
PI: J.C. Han at Texas A&M University
- Part II: Stationary Heat Transfer: Focuses on the effect of coolant-to-wall
temperature ratio
PI: Phil Ligrani at University of Utah
- Part III: Numerical Prediction: Focuses on the effect of high Reynolds number
and high buoyancy parameter
PI: H.C. Chen at Texas A&M University
- Industrial Advisors: Boris Glezer and Hee-Koo Moon - Solar Turbines
Ron Bunker - G.E. R&D Center
Ed North - Siemens Westinghouse Power
Fred Soechting - Pratt & Whitney

Part I – Rotating Heat Transfer



Orientation of a 4:1 aspect ratio channel in a gas turbine blade

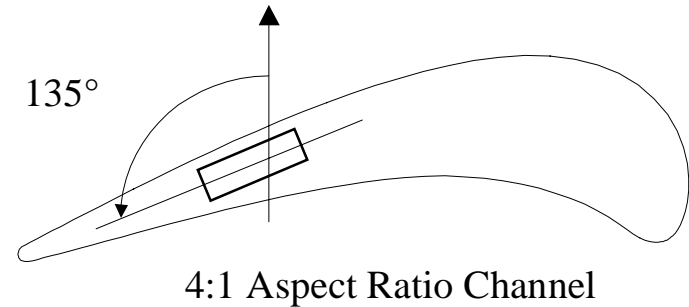


Annotation and data legend for surfaces within the 4:1 channel ($\beta = 135^\circ$)

Part I - Rotating Heat Transfer Experiment: This Work

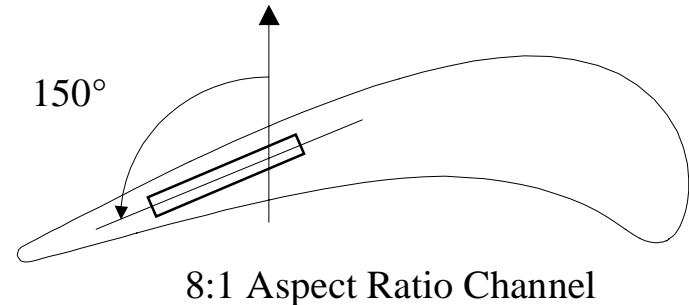
1. 4:1 Aspect Ratio Rectangular Channel

- With smooth walls
- With 45° angled ribs on leading and trailing walls
- With dimples on leading and trailing walls
- Channel orientation
- Varying inlet geometry



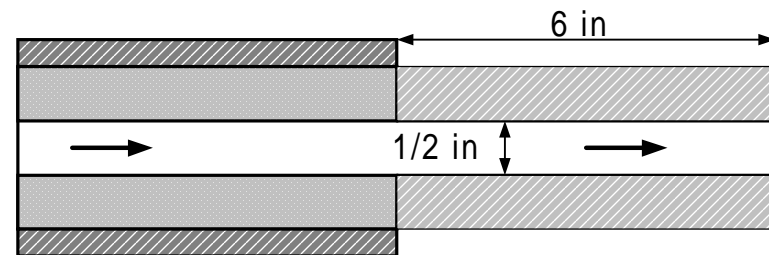
2. 8:1 Aspect Ratio Rectangular Channel

- With smooth walls
- With dimples on leading and trailing walls
- With pin-fins from leading to trailing walls
- Channel orientation
- Varying inlet geometry

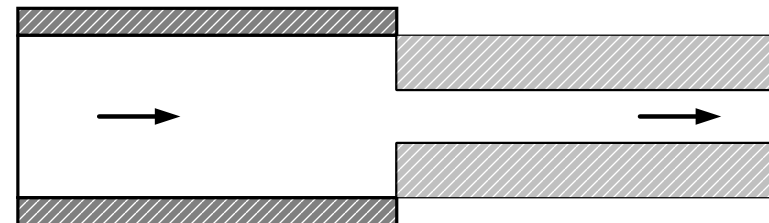
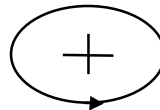


Part I - Rotating Heat Transfer Experiment: Test Section Inlet Configurations and Flow Conditions

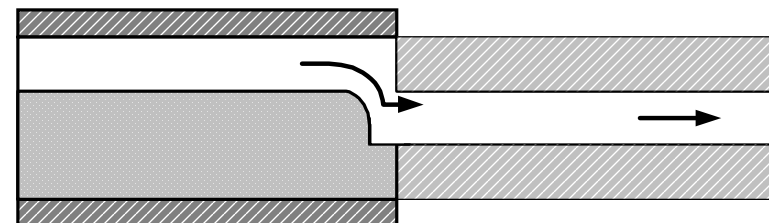
- **Fully Developed Flow**
(Radially Outward Flow)



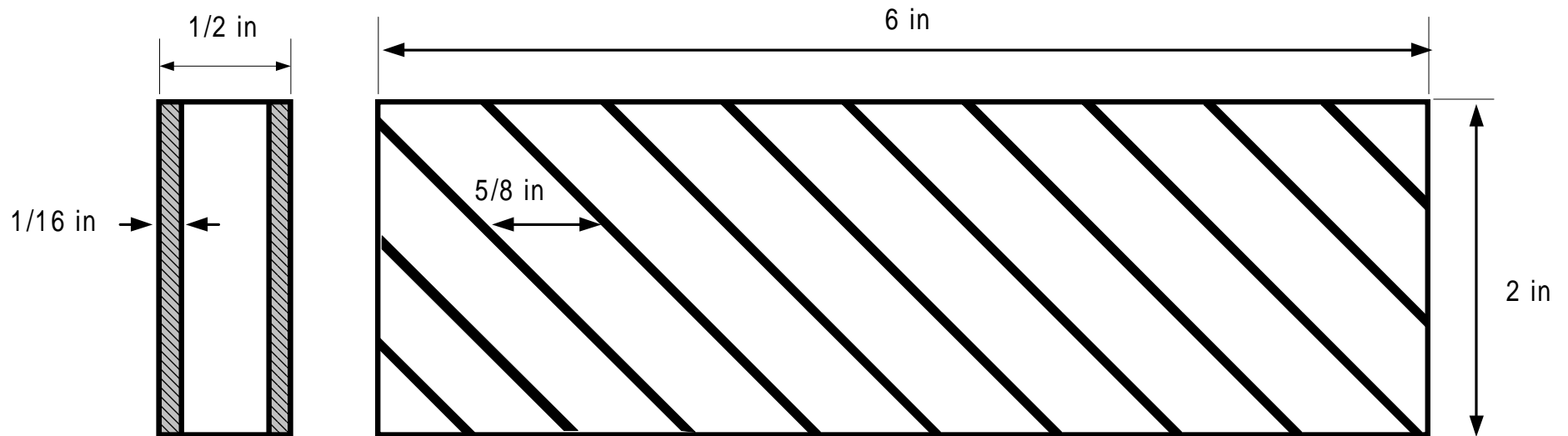
- **Sudden Contraction Flow**
(Radially Outward Flow)



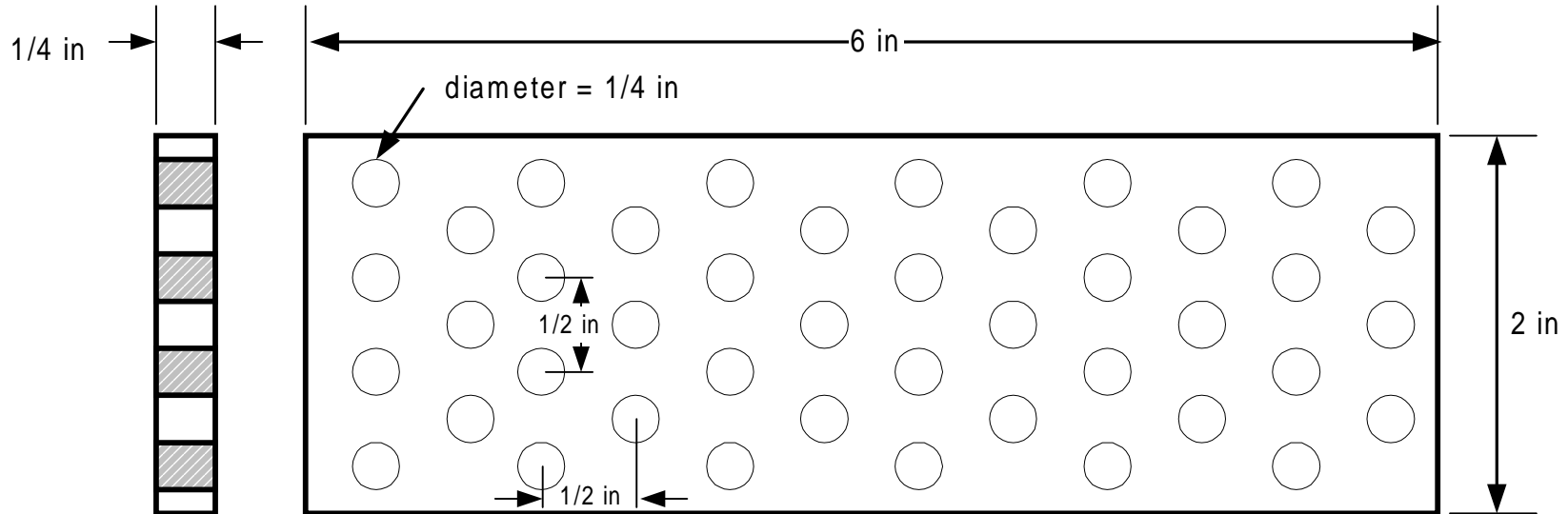
- **Partial Sudden Contraction Flow**
(Radially Outward Flow)

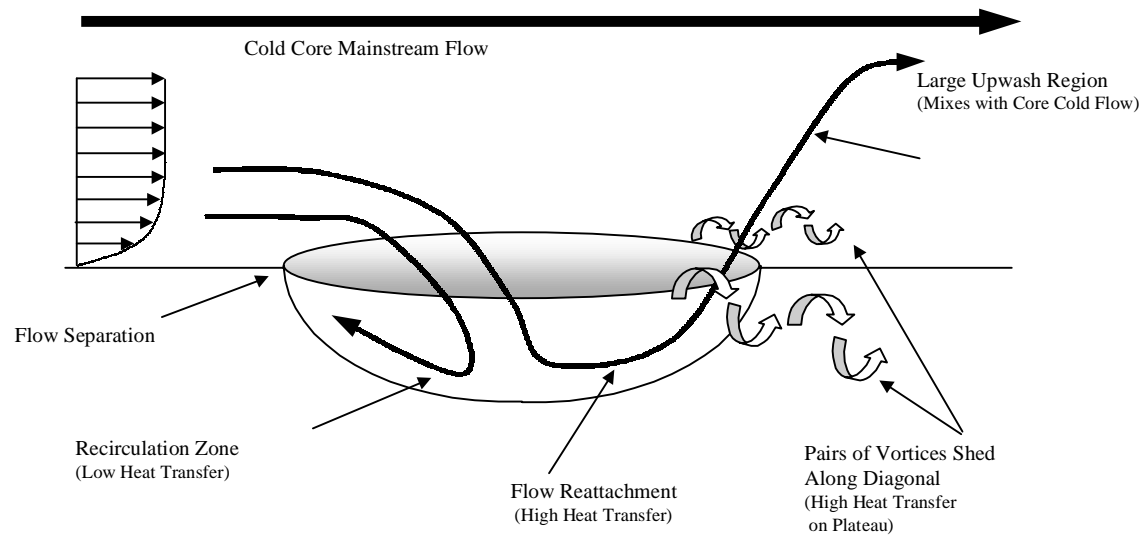
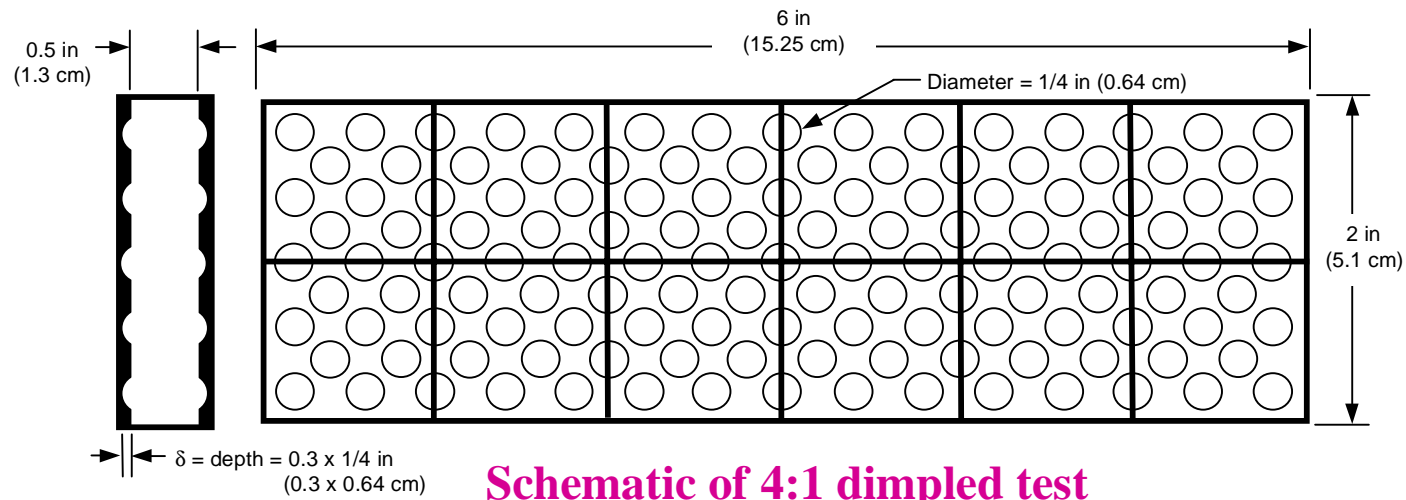


Part I - Rotating Heat Transfer Experiment: 4:1 Aspect Ratio Channel with Ribs

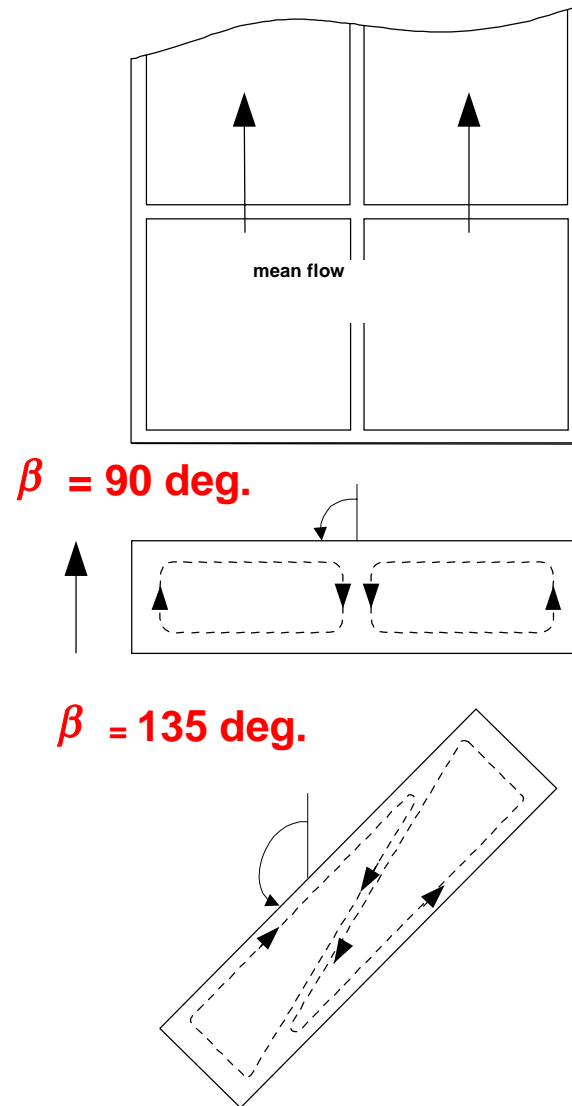


Part I - Rotating Heat Transfer Experiment: 8:1 Aspect Ratio Channel with Pins

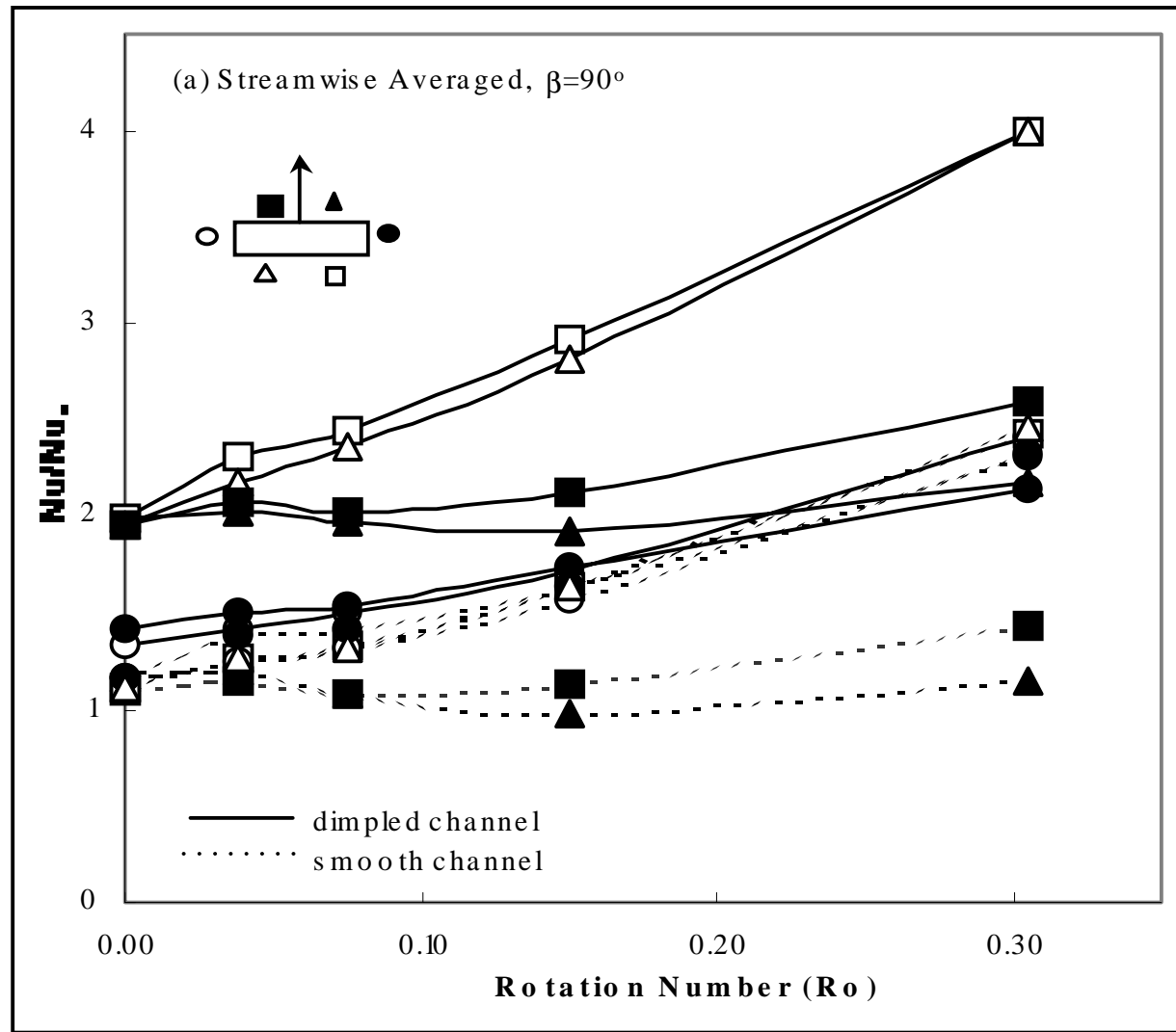




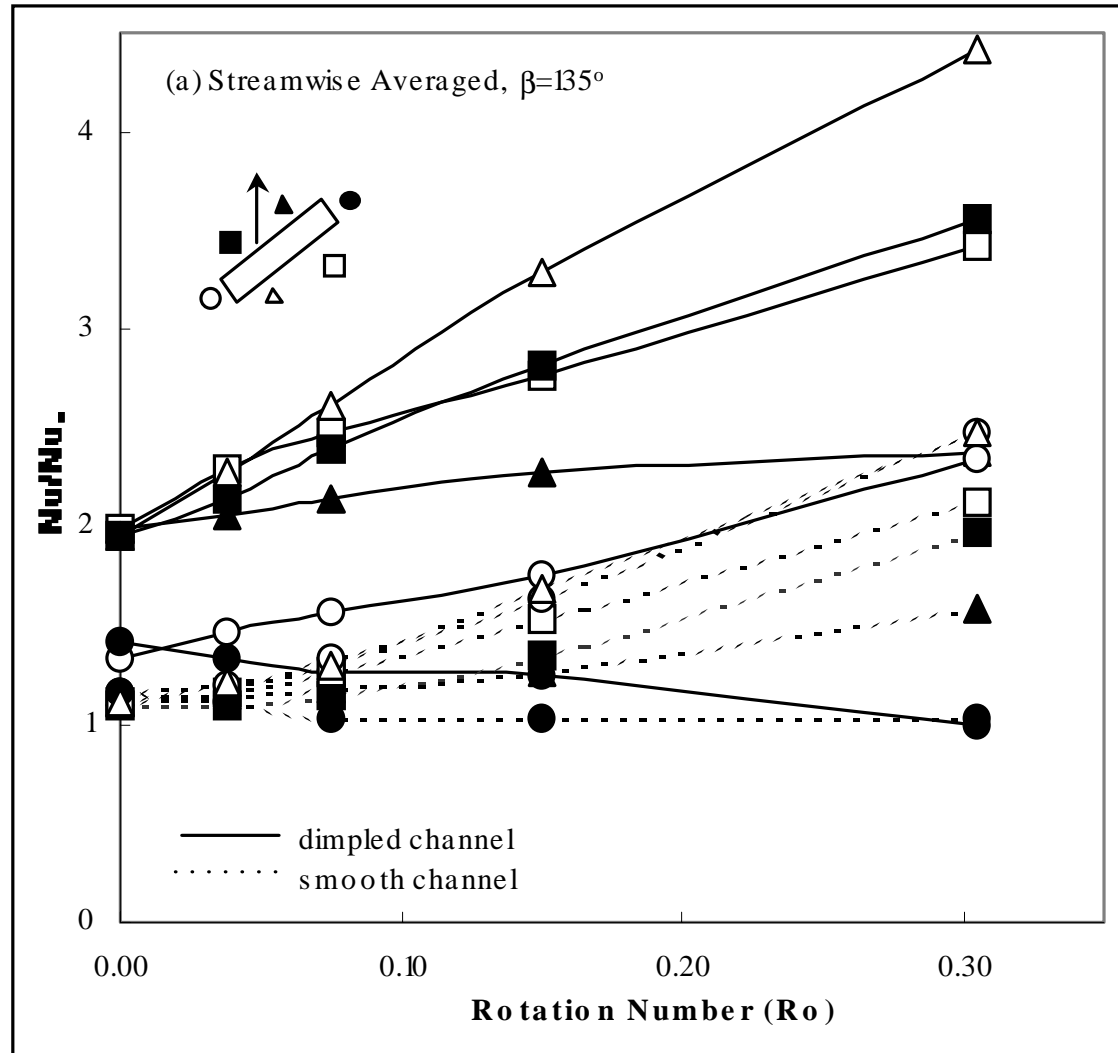
**Dimple induced secondary flow
(conceptualization)**



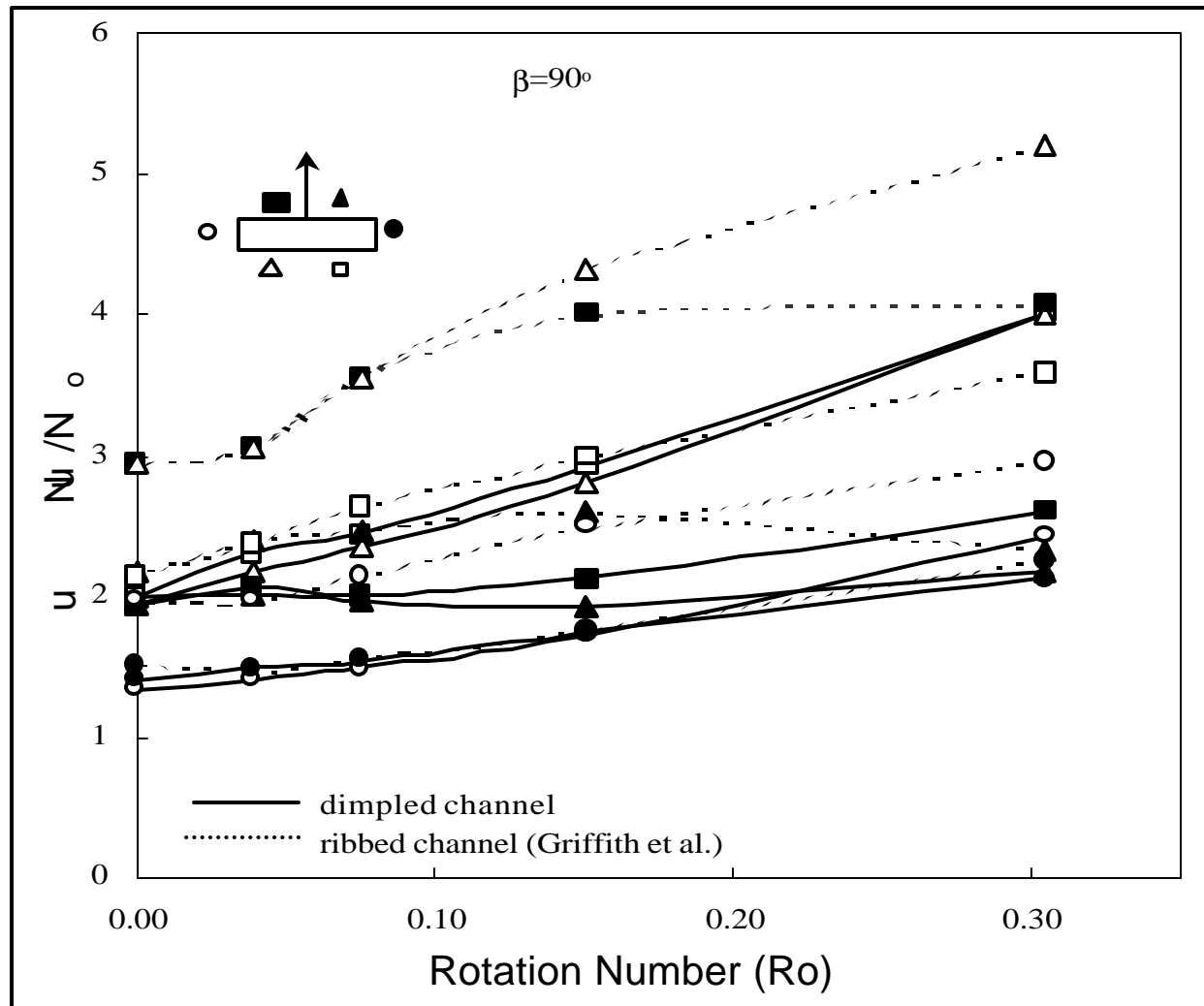
Rotation-induced (Coriolis force) vortices in rectangular channel



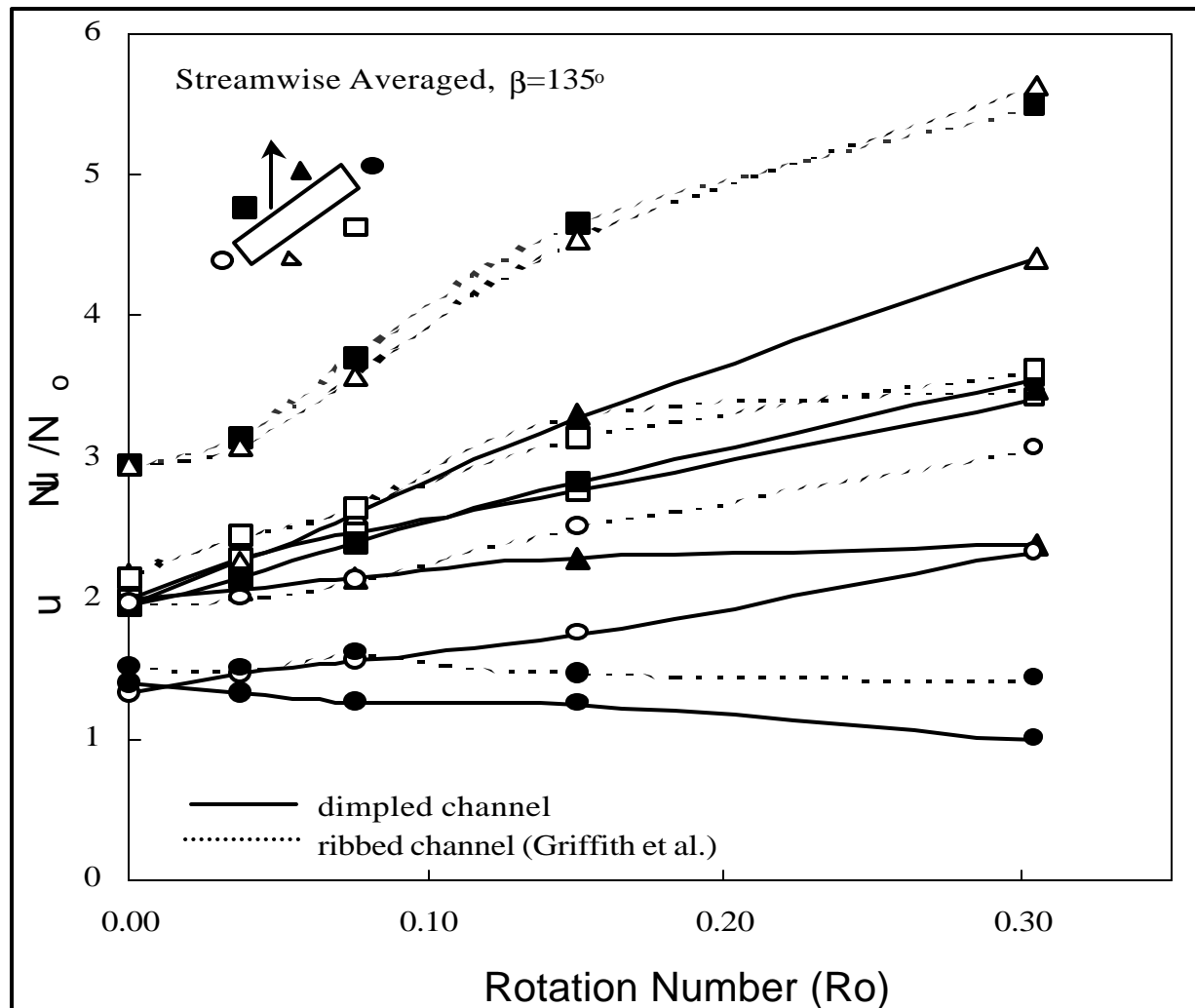
Streamwise Averaged Nusselt number ratio for smooth and dimpled channel with $\beta = 90^\circ$



Streamwise averaged Nusselt number ratio for smooth and dimpled channel with $\beta = 135^\circ$



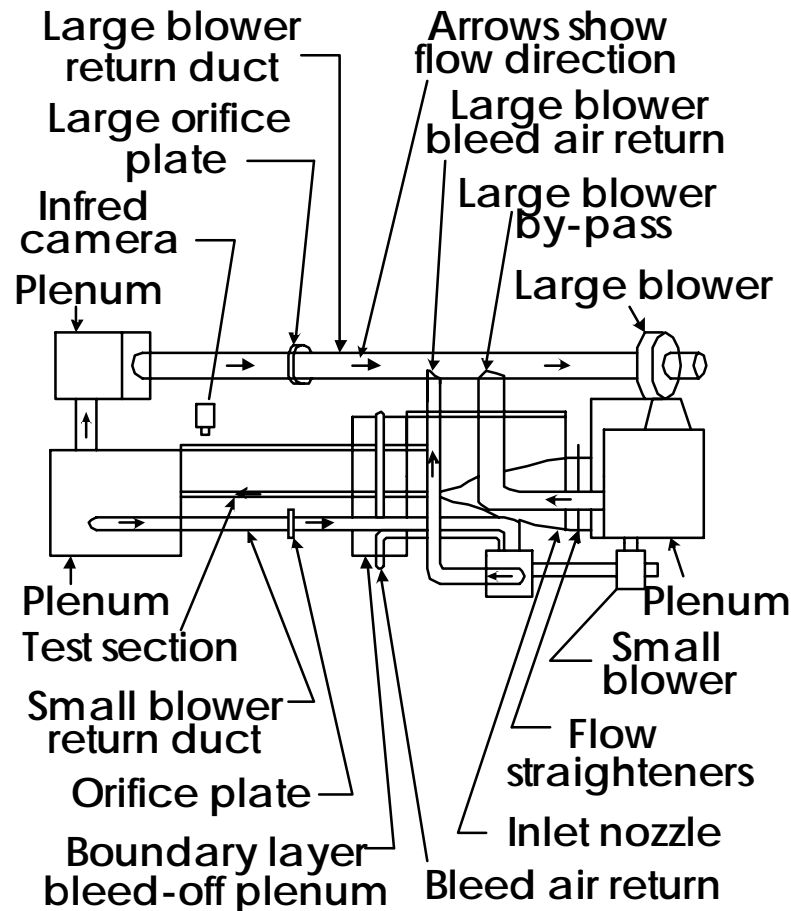
Streamwise Averaged Nusselt Number Ratio for
Dimpled and Ribbed Channels with $\beta=90^\circ$



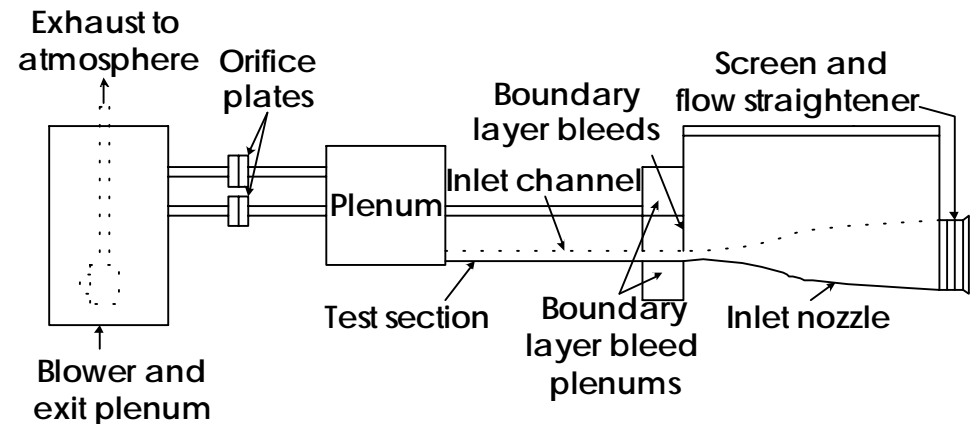
Streamwise Averaged Nusselt Number Ratio for
Dimpled and Ribbed Channels with $\beta=135^\circ$

Part II

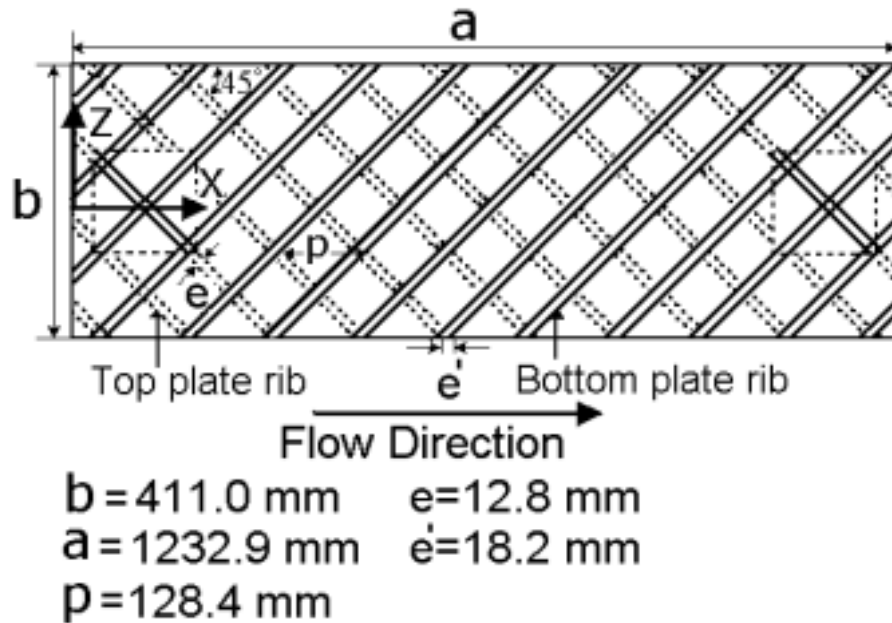
Stationary Heat Transfer (University of Utah)



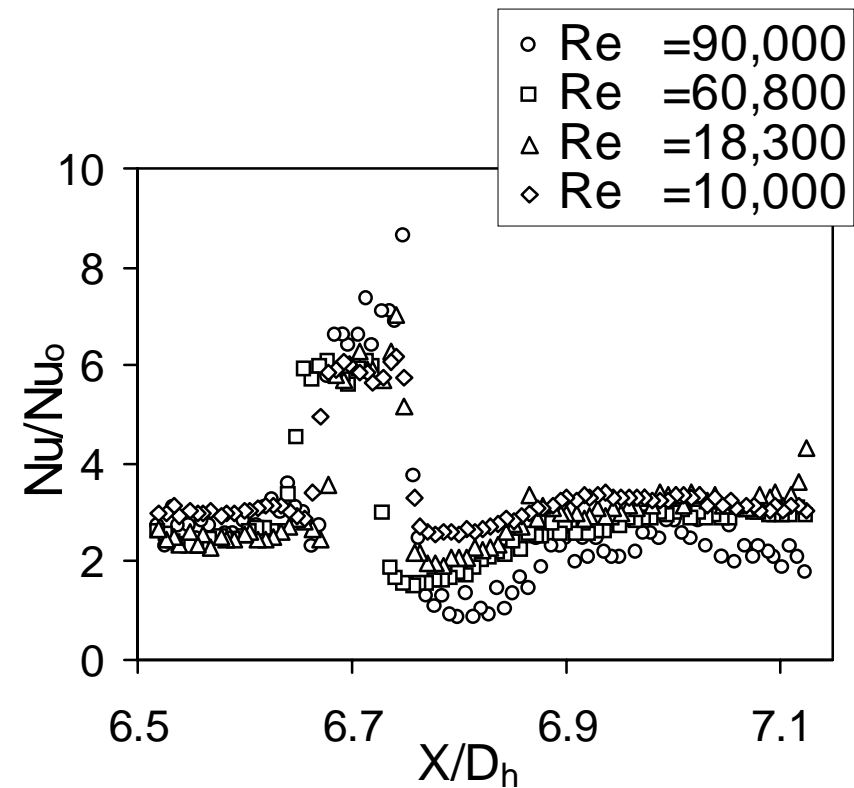
- **Experimental apparatus used for heat transfer measurements**



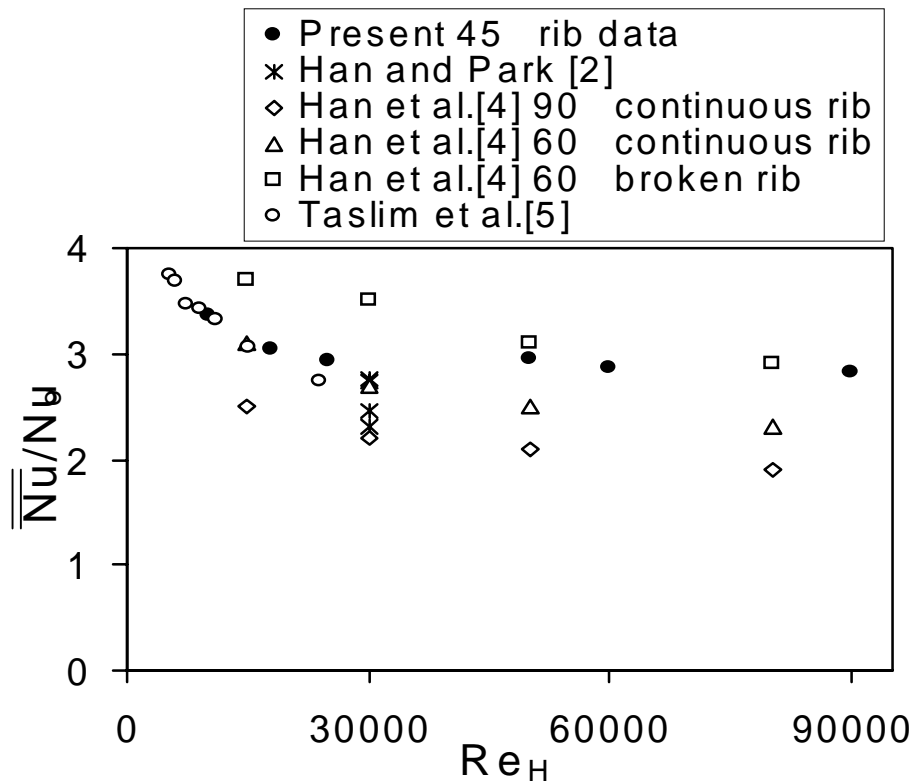
- (b) **Experimental apparatus used for flow visualizations and measurements of flow structure**



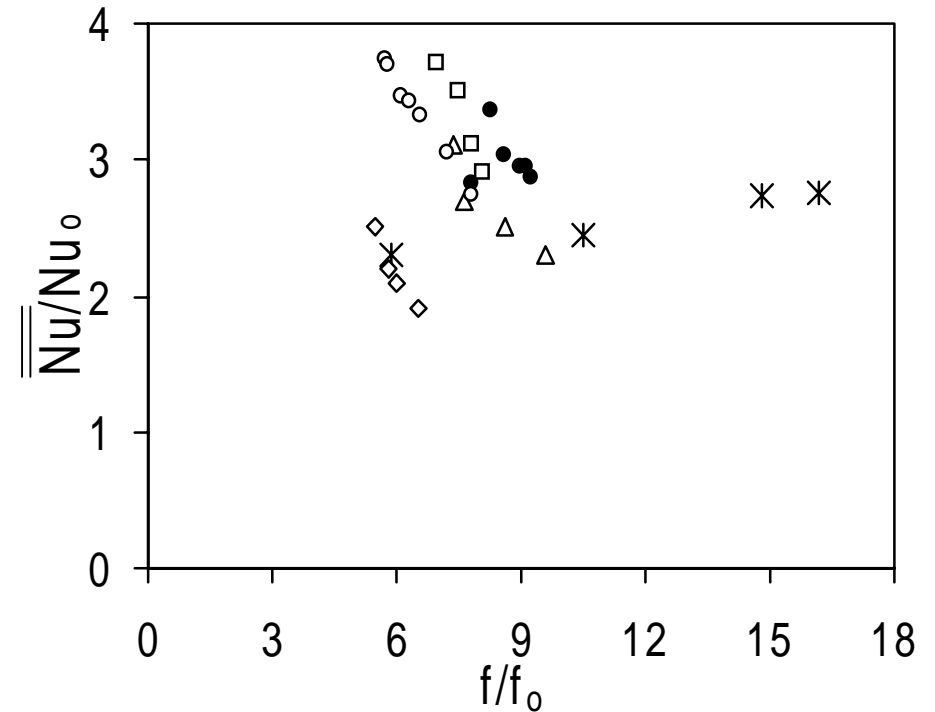
**Schematic diagram of the rib
turbulator test surfaces,
including coordinate system**



**Local Nusselt number ratios
along the rib turbulator test
surface at $\phi = 0.0$ for different
Reynolds numbers Re_H and
of 0.93-0.95**



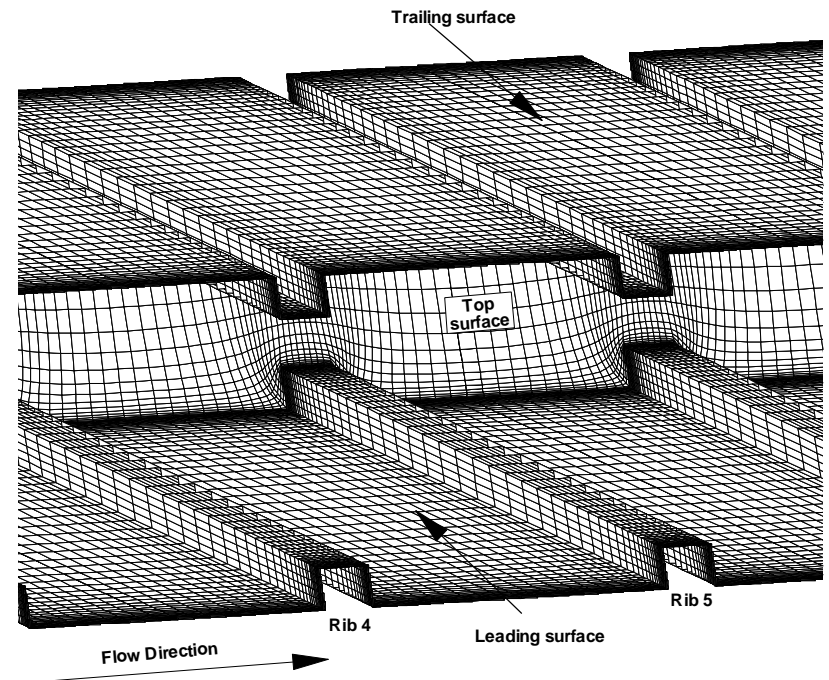
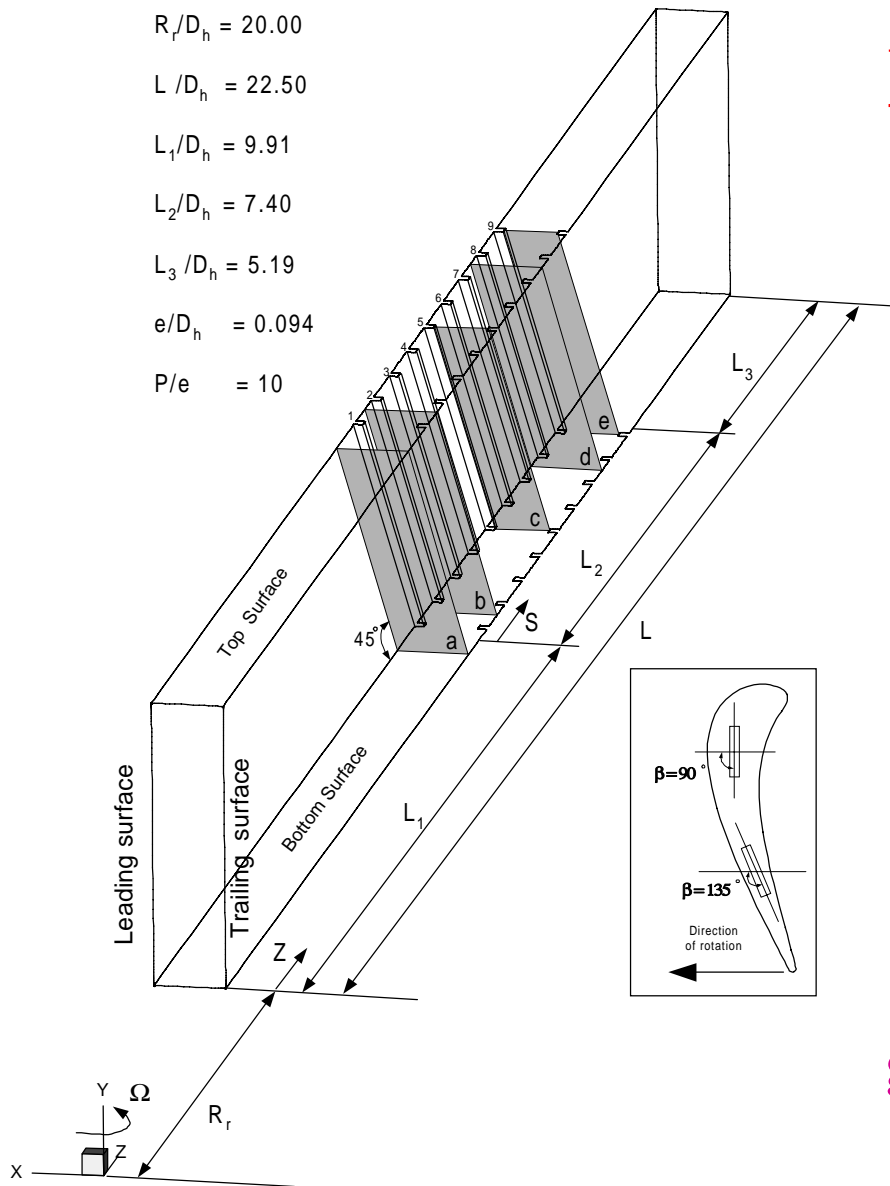
Rib turbulator channel globally-averaged Nusselt number ratios for fully developed flow, averaged over the surface area corresponding to one period of rib turbulator geometry, as dependent upon Reynolds number for =0.93-0.95.



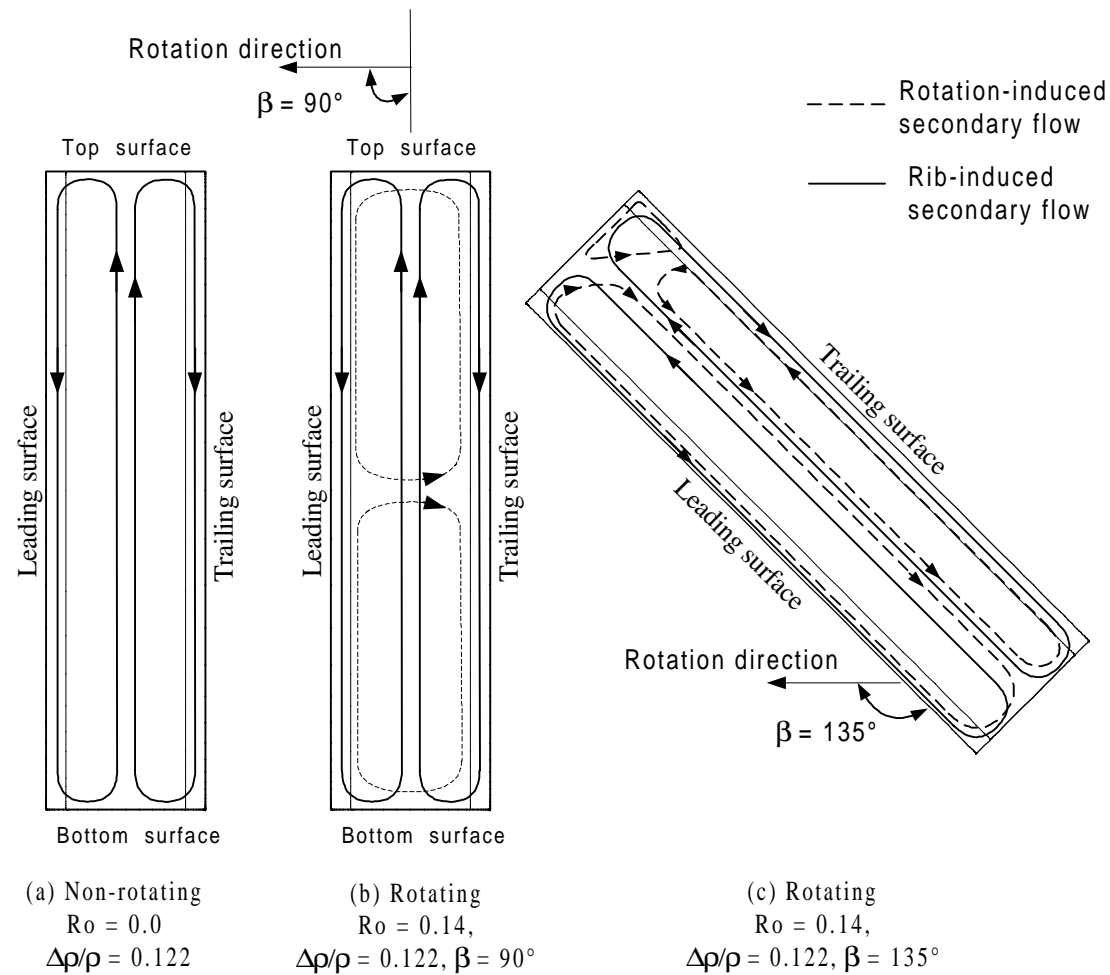
Rib turbulator channel friction factor ratios for fully developed flow conditions as dependent upon Reynolds number for =0.93-0.95.

Part III

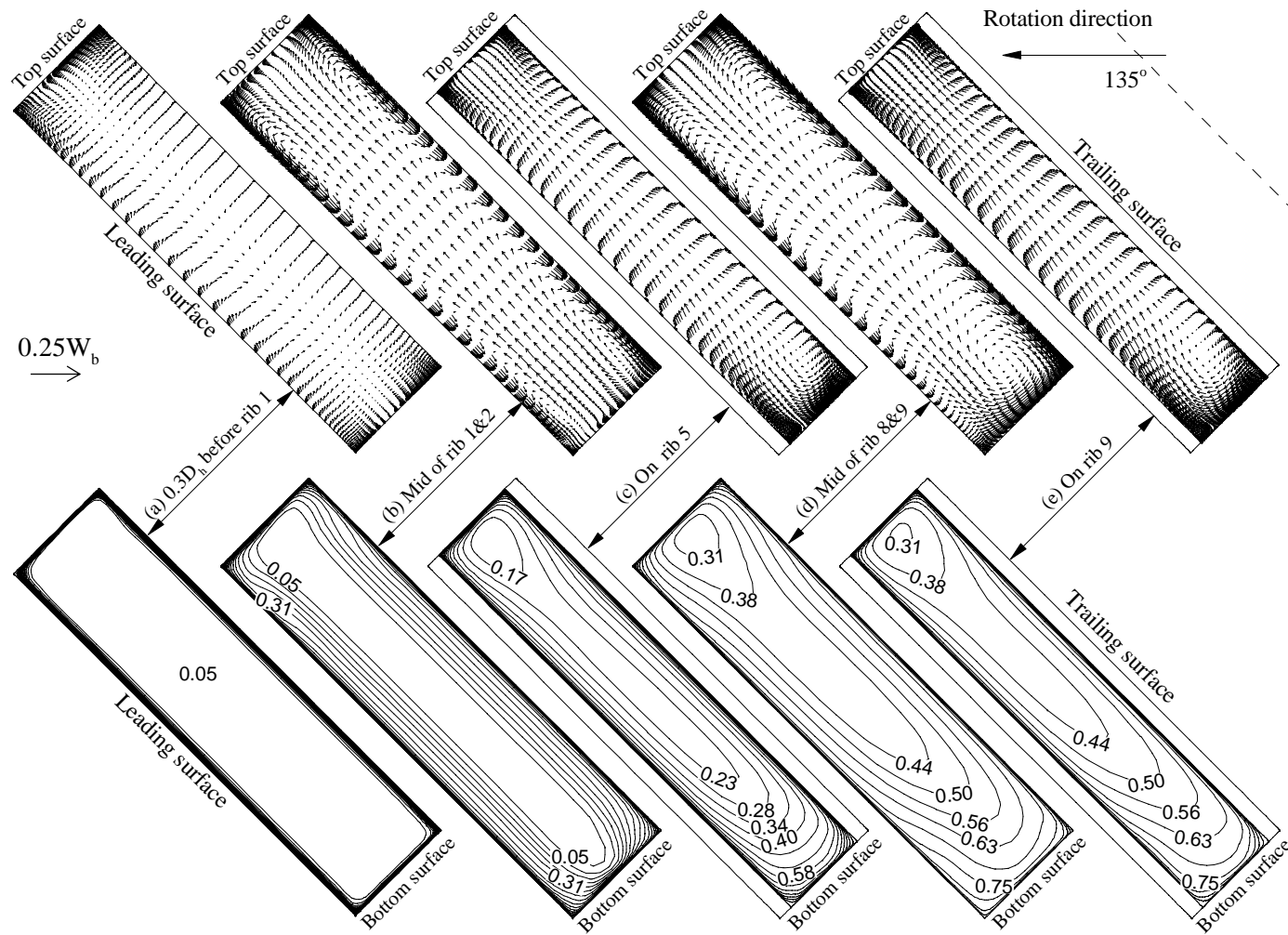
Numerical Predictions



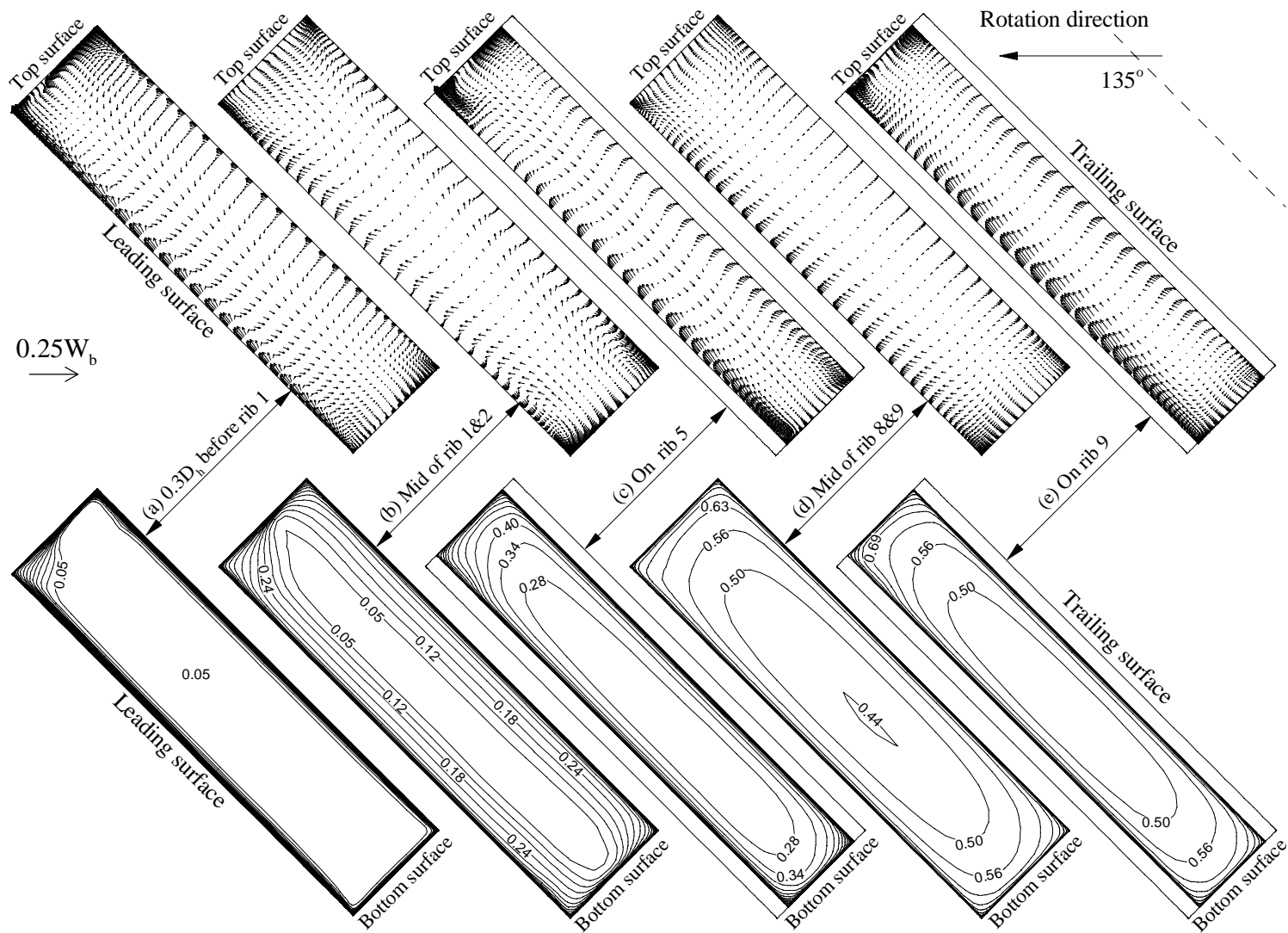
Geometry and computational grid of ribbed rectangular duct with AR = 4:1.



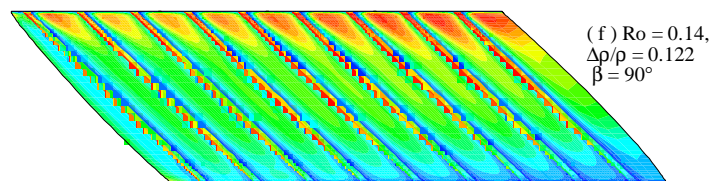
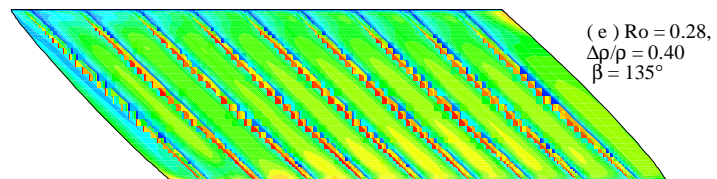
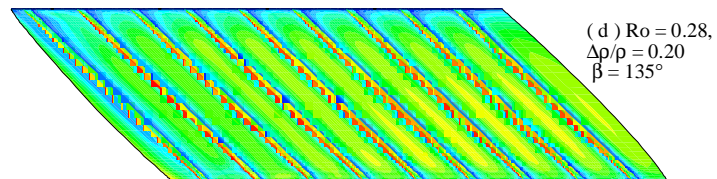
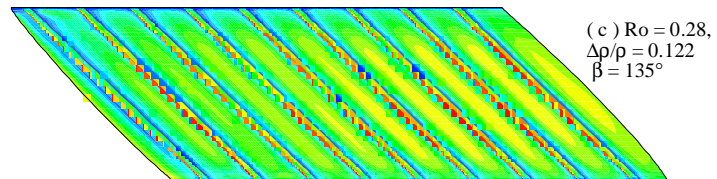
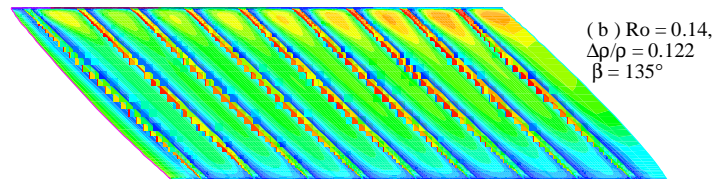
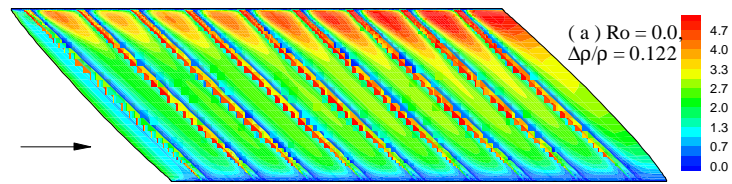
Conceptual view of the secondary flow induced by angled ribs and rotation



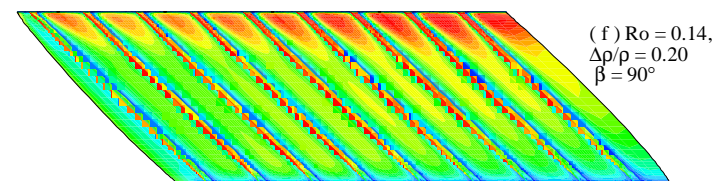
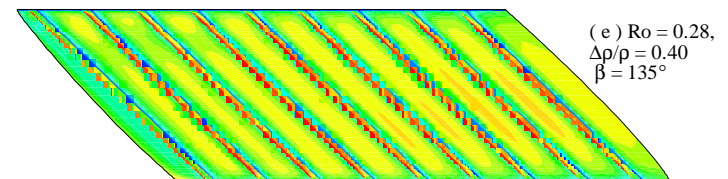
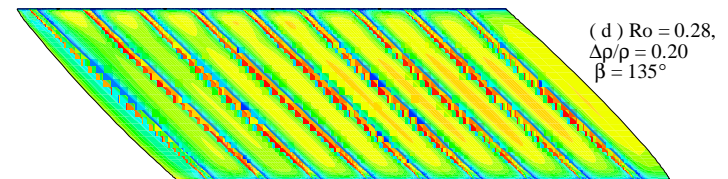
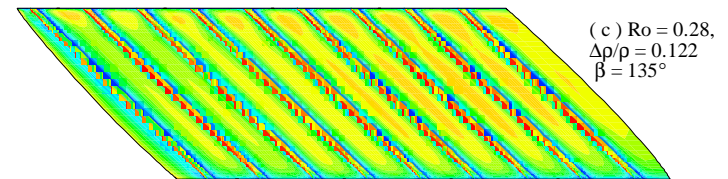
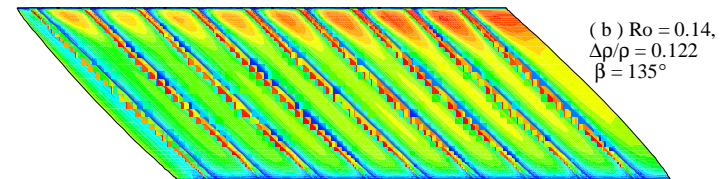
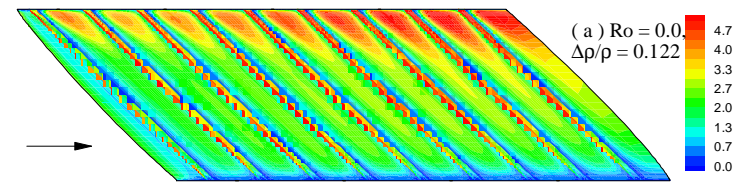
Secondary flow and temperature $[\theta = (T - T_o)/(T_w - T_o)]$ for rotating ribbed duct, $Ro = 0.14$, $\Delta\rho/\rho = 0.122$ and $\beta = 135^\circ$



Secondary flow and temperature $[\theta = (T - T_o)/(T_w - T_o)]$ for rotating ribbed duct, $Ro = 0.28$, $\Delta\rho/\rho = 0.40$ and $\beta = 135^\circ$

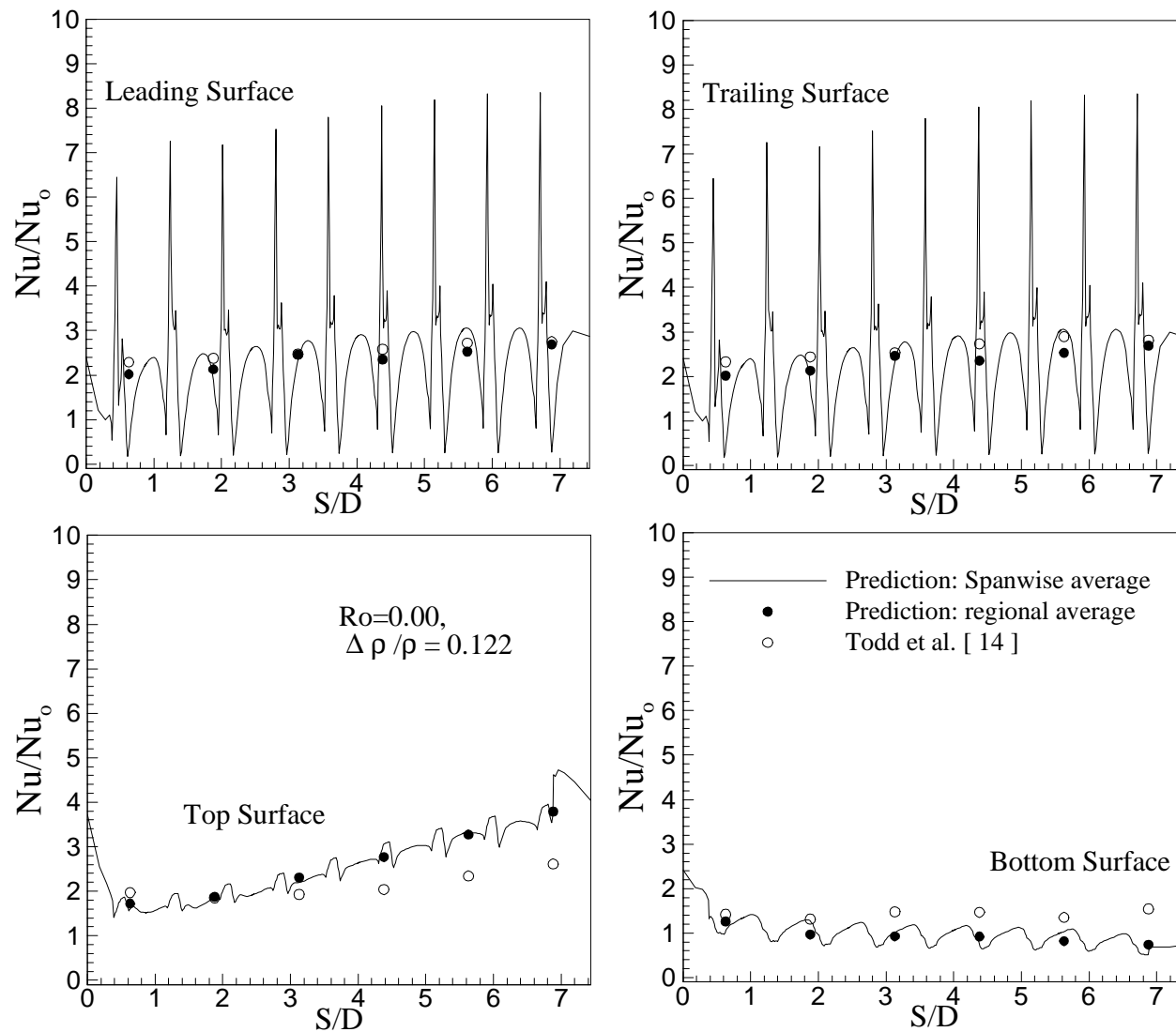


(a) Leading Surface

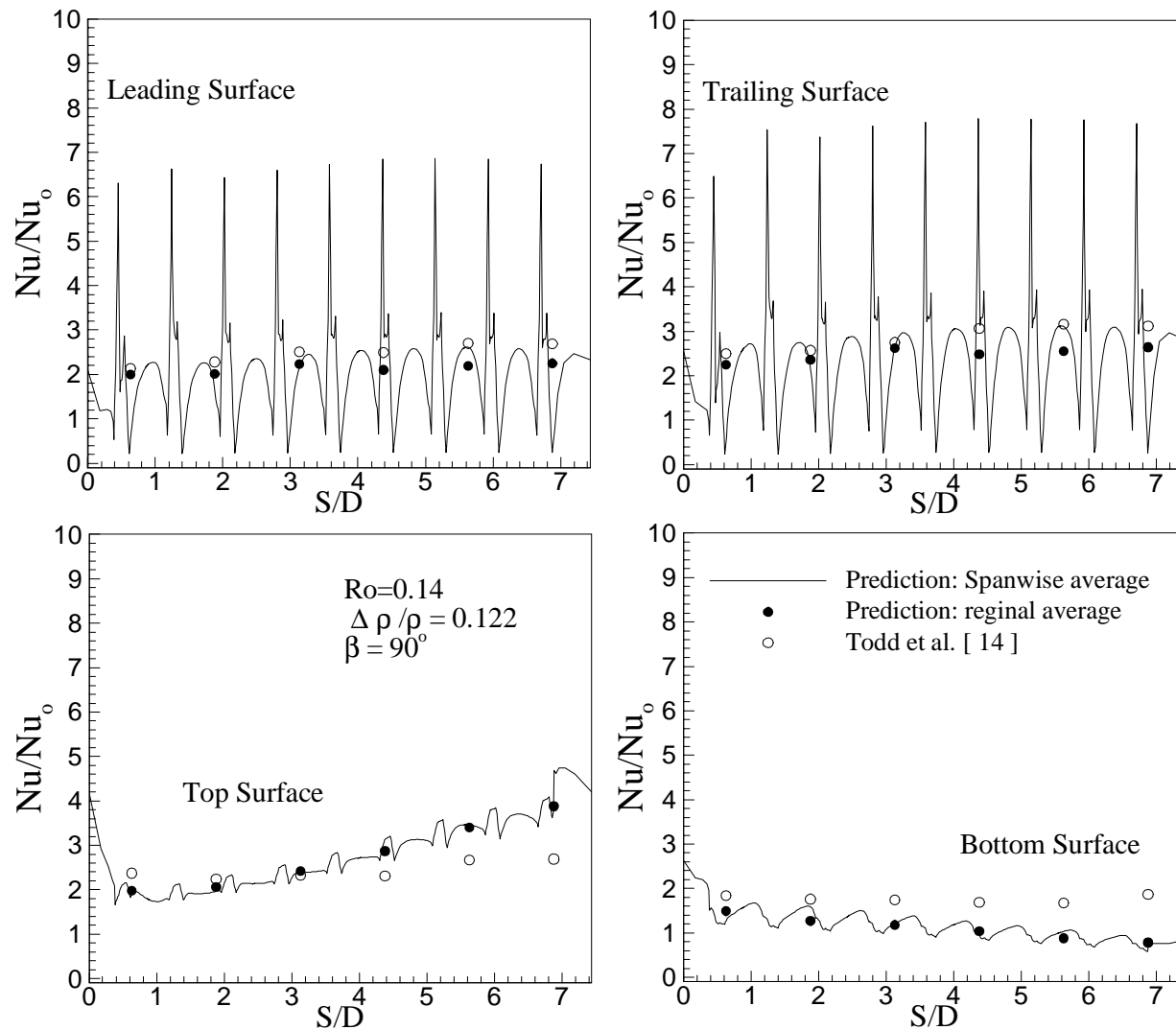


(b) Trailing Surface

Detailed Nusselt number ratio distribution in ribbed duct



**Calculated and measured Nusselt number ratio distribution
for non-rotating ribbed duct, $Re = 10,000$**



Calculated and measured Nusselt number ratio distribution for rotating ribbed duct ($Ro = 0.14$), $Re = 10,000$.

Conclusions

Part I: Rotating Heat Transfer

- Spanwise variations in heat transfer enhancement of the dimpled rotating rectangular channel exist only for the twisted ($\beta = 135^\circ$) orientation.
- The dimpled channel behaves somewhat similarly to the ribbed channel. The dimpled channel however, does not dominate the rotational effects quite as significantly as in the ribbed channel. It appears that the dimpled channel promotes smaller scale, and more complex mixing vortices than the ribbed channel.
- The twisted ($\beta = 135^\circ$) dimpled channel experiences greater overall enhancement than the orthogonal dimpled channel ($\beta = 90^\circ$).
- For ($\beta = 90^\circ$), enhancement at the trailing surfaces increases by almost 100% from the stationary to highest rotation number case. Also, the leading surfaces show little dependence on rotation number. The side surfaces show slightly less dependence on rotation than those of a smooth duct.
- For ($\beta = 135^\circ$), enhancement at the trailing-outer surface increases by more than 100% from the stationary to highest rotation number case. In addition, the trailing inner and leading outer surfaces experience nearly identical enhancement, increasing by more than 50% from the stationary to highest rotation number case. The outer surface increases by nearly 100% and the inner surface slightly decreases from the stationary to highest rotation number case.

Conclusions

Part II: Stationary Heat Transfer and Flow Field

- Globally-averaged Nusselt number ratios vary from 3.36 to 2.82 as Reynolds number increases from 10,000 to 90,000. Thermal performance parameters also decrease somewhat as Reynolds number increases over this range. Such performance parameter magnitudes and Nusselt number variations are due augmented three-dimensional turbulence transport and increased secondary flow advection, as well as the pressure losses and friction factors produced by the form drag which develops around the rib turbulators.

Part III: Numerical Prediction

- The present near-wall second-moment closure model results predicted fairly well the complex three-dimensional flow and heat transfer characteristics resulting from the large channel aspect ratio, rotation, centrifugal buoyancy forces and channel orientation.
- The effect of increasing the rotation number (with fixed density ratio) is to monotonically increase the Nusselt number ratio on the trailing surface.
- The effect of increasing the density ratio (with fixed rotation number) is to have higher and uniform Nusselt number ratio on the leading and trailing surfaces.
- From design point of view, it is clear that the rib angle and the direction of rotation should be chosen such that the secondary flows that are induced by the rib angle and rotation direction should combine constructively to give maximum heat transfer.

Ongoing Work

Part I: Rotating Heat Transfer

- Dimple plates of three different dimple depths (10%, 20%, and 30% of dimple diameter) have been manufactured using a CNC mill.
- Acrylic pins have been obtained for the pin-fin experiments. These experiments are currently underway to obtain the effect of rotation on the cooling channel with pin fins.
- Stationary pressure drop experiments are completed to determine the pressure drop in three different dimple depths (10%, 20%, and 30% of dimple diameter). The test section is made of acrylic and will later be used for liquid crystal thermography experiments.

Part II: Stationary Heat Transfer and Flow Field

- Heat transfer measurements (at one temperature ratio and different Re): The rib turbulators are completed, the pin fins are almost completed. Also, the dimples are scheduled for the near future.
- Heat transfer measurements (at different temperature ratios and one Re): The rib turbulators are completed, and the pin fins are almost done. The dimples are scheduled for the near future.

Part III: Numerical Prediction

- Calculations of flow field, heat transfer coefficients, and pressure drops is currently being performed for the pin fin configurations under various combinations of rotation number, coolant to wall temperature ratio, and channel orientation.
- Calculations of flow field, heat transfer coefficients, and pressure drops will be performed for the dimple configuration under various combinations of rotation number, coolant to wall temperature ratio, and channel orientation.